

# 2D-DEM modelling of the formwork removal of a rubble stone masonry bridge

Tran, V. H. , Vincens, E. , Morel, J. C. , Dedecker, F. and Le, H. H.

**Author post-print (accepted) deposited in CURVE February 2016**

**Original citation & hyperlink:**

Tran, V. H. , Vincens, E. , Morel, J. C. , Dedecker, F. and Le, H. H. (2014) 2D-DEM modelling of the formwork removal of a rubble stone masonry bridge. Engineering Structures, volume 75 : 448-456

<http://dx.doi.org/10.1016/j.engstruct.2014.05.048>

ISSN 0141-0296

DOI 10.1016/j.engstruct.2014.05.048

**Copyright © and Moral Rights are retained by the author(s) and/ or other copyright owners. A copy can be downloaded for personal non-commercial research or study, without prior permission or charge. This item cannot be reproduced or quoted extensively from without first obtaining permission in writing from the copyright holder(s). The content must not be changed in any way or sold commercially in any format or medium without the formal permission of the copyright holders.**

**This document is the author's post-print version, incorporating any revisions agreed during the peer-review process. Some differences between the published version and this version may remain and you are advised to consult the published version if you wish to cite from it.**

# 2D-DEM modelling of the formwork removal of a rubble stone masonry bridge

VH. Tran<sup>1</sup>, E.Vincens<sup>2</sup>, JC. Morel<sup>1</sup>, F. Dedecker<sup>3</sup>, HH Le<sup>1</sup>

1 Université de Lyon, LTDS, UMR CNRS 5513, LGCB ENTPE, 3 rue Maurice Audin, 69518 Vaulx en Velin Cedex, France

2 Université de Lyon, LTDS, UMR CNRS 5513, Ecole Centrale de Lyon, 36 avenue Guy de Collongue, 69134 Ecully Cedex, France

3 Itasca Consultants, S.A.S., 64 Chemin des Mouilles, 69134 Ecully Cedex, France

Corresponding author: E. Vincens

Phone: +33 6 79 88 02 24

Email: eric.vincens@ec-lyon.fr

## Abstract

This study aims to determine the mechanical behaviour of a stone arch bridge during the phase of the formwork removal. This operation is the most delicate during construction, because it puts in charge the arch which must work in compression for stability. On-site measurements of the displacement of the arch voussoirs during the process of the formwork removal were carried out. Then, some mechanical tests were performed with the stones used in the construction to determine the mechanical properties required for modeling the structure by a discrete element method. This numerical approach has the ability to find the specific pattern of the displacement field observed on-site that could not have been found with a finite element method. The key feature is the rotation of the voussoirs which changes the location of the zones of contact from one to another. Therefore, the contacts from one to another are restricted to a small zone for the voussoirs close to the keystone.

**Key Words:** masonry bridge, arch, stone, dry joint, on site measurements, DEM.

## 1. Introduction

While steel or reinforced concrete bridges have been under development only over the last century, masonry bridges have kept their ability to cross valleys and rivers for centuries. The key element in these stone-structures is the arch that transfers both vertical and horizontal loadings toward its basement. The arch is composed of stones usually with dry thin joints kept into equilibrium by compressive forces, but also thanks to friction acting between the blocks. To resist to a high level of compressive stresses and to avoid the possibility of alteration over time, the stones must be chosen carefully.

The durability of bridges is intimately related to the quality of the maintenance. But, the feedback shows that if the initial choice of the material was properly done, the stone bridges can be maintained over time without frequent intervention. This is not the case of steel or reinforced concrete bridges. The “pont du Gard,” a stone bridge that is actually an aqueduct, was built by the Romans during the first century in the south of France, and is an outstanding example of such durability. Actually, this

resistance over time was made possible by an over design of the structure, which compensates the use of a relatively weak material.

The new interest of French authorities in stone bridges is due to the decades of neglect, though such structures represent 40% of highway-bridges on French high-traffic roads. The concern of the authorities in charge of this maintenance is the difficulty in making a decision when problems have appeared in such structures. Indeed, the precise forecast of their behaviour cannot be provided by usual numerical tools in critical loading situations due to the nature of the system. The hypothesis of a continuum system is broken due to the discrete nature of system, because large deformations can be generated by movements of blocks without jeopardizing the overall stability of the structure.

Taking advantage of the construction of a new stone arch bridge in the Cévennes (south of France), some on-site measurements were performed at the stage of the wooden formwork removal. A simulation of this process was performed to evaluate the capacity to model and forecast the behaviour of such a complex system. This work is just a first-step before the modelling of this stone bridge behaviour against life service loadings and extreme loadings is able to trigger failure.

This single span highway bridge called Chaldecoste Bridge was built in the district of Saint-Andéol-de-Clerguemort, which belongs to the Natural Park of Cevennes. This type of bridge was chosen by the local authorities to replace an old crossing composed of a flume and cyclopean concrete that was destroyed during a flood in 2008. The concern was how to insert the new bridge without complications into the preserved scenery of the Natural Park. A building technology that had widely been used in the past was chosen for this task. In this region, many of the bridges that were built since the beginning of the 18<sup>th</sup> century are stone bridges with weakly bound schist blocks that were extracted from local stone quarries.

The span length of the arch bridge is 6 m and the width is 4.8 m. The blocks that vary in size and shape are bound by a lime mortar. This mortar plays a role of filling the voids within the joints between the blocks in contact. This mortar was recommended for preventing water flow between the blocks, which could alter the durability of the structure.

Different approaches can be taken to model this kind of structure according to the level of complexity one may expect to solve the problem. In the literature and considering the nature of the system, there are mainly four methods that can be found. The first one is the rigid block limit analysis [1-3], which is suitable when the study focuses on the ultimate loading of a system at failure. There is no access to the deformation field. The second one is the finite element method where the whole structure is continuous [4-9]. This approach is usually suitable for a system composed of individual bodies when deformations are not too large. Nevertheless, the use of a damaging model (propagation of cracks possible) or joints in pre-identified zones allows the failure behaviour to be studied. Thus, a large strain field is reachable. The third method is the use of a discrete element method (DEM) involving specific contact laws between distinct objects [10-14]. This method allows the failure behaviour of the structure to be studied more accurately.

In the case of loadings generating small deformations, a finite element method is suitable to address the problem since the global behaviour of the structure is supposed to remain in the elastic domain. This is the case for modelling the formwork removal, because only small deformations are expected. Nevertheless, a DEM approach is chosen for the overall study, because in a forthcoming study, the behaviour of the bridge will be simulated under service loadings and against loadings that are able to lead to failure where high dissipation energy can take place.

In the first part, the measurements of the arch displacement field performed on-site during the formwork removal are presented. In a second part, the laboratory tests are presented. They were performed to identify the properties of the different materials that constituted the stone arch bridge and the spandrel walls. It will help for the determination of the mechanical parameters required for a DEM modelling of the structure. Finally, the modelling of the formwork removal and specially the resulting vertical displacements of the voussoirs are given and compared to the measurements performed on-site.

## 2. On-site measurement of displacements of the arch during the formwork removal

### 2.1. Implementation of measurements

The measurements are carried out by means of the laser ray device Leica Absolute Tracker AT401, which is a portable system tool distance measuring (CMM) with an accuracy of  $\pm 10\mu\text{m}$  over a distance of 320 m. A computer with the Pilot Tracker software is also connected to the device, which enables control of both the measuring device and recording measurement. Twelve optical reflectors are positioned at the points where information is expected. Reflectors 1 to 10 are installed on the arch facing, while reflectors 11 and 12 are installed on the spandrel walls as reference points. Figure 1 shows the positions of the reflectors on the structure. The position of reflectors 11 and 12 are not showed in this figure, but only in the figure 2. The position of the reflectors is measured before and after the formwork removal, twice each time for better accuracy. The results are three-dimensional coordinates of the reflectors, presented in the coordinate system of the laser measurement system.

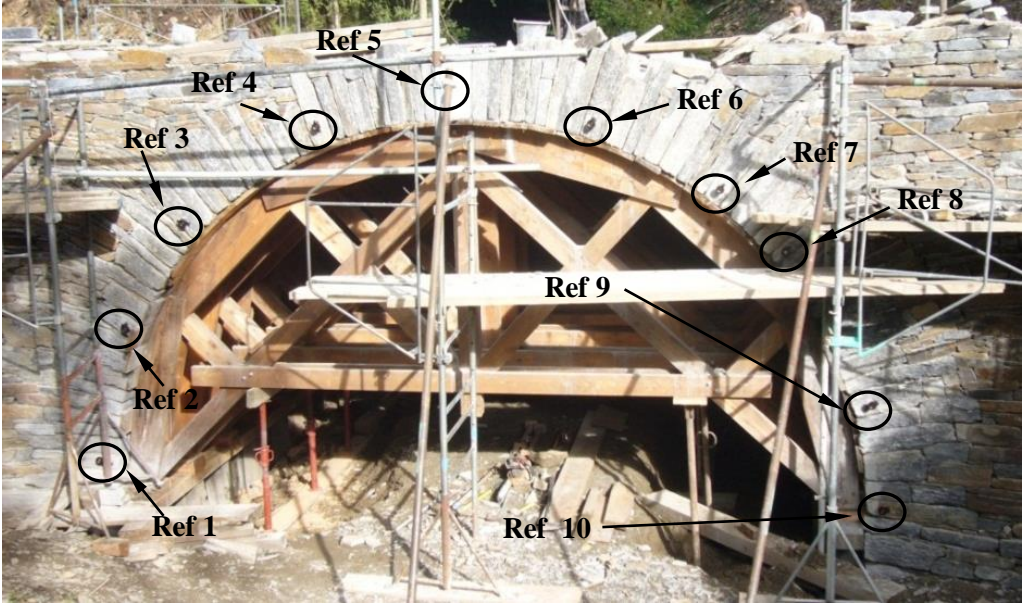


Figure 1 : Position of the reflectors from 1 to 10 on the arch voussoirs before the test. The picture was taken before the test (the formwork is not yet removed).

## 2.2. Reconstruction of the shape of the arch

The on-site measurements obtained are performed with respect to the coordinate system of the measuring tool. Considering that the measuring points are in the plane of the spandrel walls where points 11 and 12 are located, we established a new coordinate system (Oxyz), where the origin 'O' represents the reference point 11 on the left hand spandrel wall (Figure 2). For each reflector (1 to 10), a point at the edge of the arch is measured while installing the reflectors. Considering the measuring points or reflector points as the center of a circle, small circles are plotted in such a way that the circle radius is equal to the distance between the reflector point and the edge of the arch (see Figure 2). The curve tangent to the small circles draws a large semi-circle, which is considered as the intrados of the vault. The extrados is very irregular as shown in Figure 1 and the imbrication of blocks with the spandrel wall does not facilitate the identification of this entity. At the location of the keystone, the position of the extrados is clear, which is not the case for the envelope closer to the haunches (Figure 3). Then some hypotheses must be settled for the location of the extrados in the modelling. Given Figure 3, an estimate of the arch thickness at springing level is two to three times of that which is observed at the keystone. According to the arch reconstruction from observations, the diameter of the intrados semicircle is 5981 mm, while for construction it was considered to be 6000 mm.

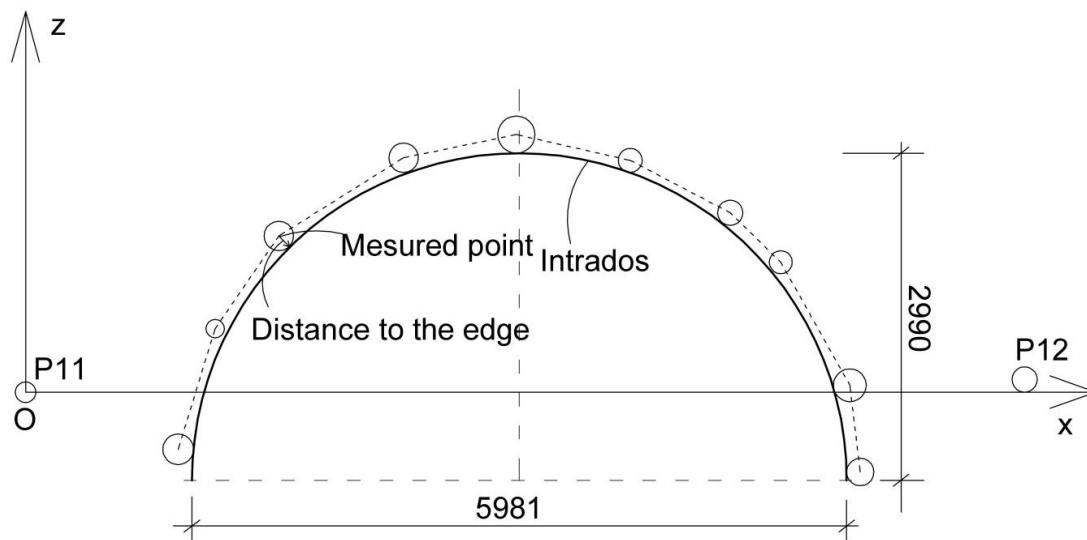


Figure 2: Shape of the rebuilt arch according to the measured points.



Figure 3: Focus on the haunches of Chaldecoste Bridge (Photo credit: P. Mc Combie)

### 2.3. Calculation of the displacements of the arch

After calculating the coordinate points in (Oxyz) coordinate system and neglecting the displacement in the direction perpendicular to the plane of the bridge, the displacement of the points due to the formwork removal is determined. Figure 4 depicts the position of the reflector points before and after the formwork removal. In this figure, the displacements are multiplied by 1000 for a better perception of the phenomena.

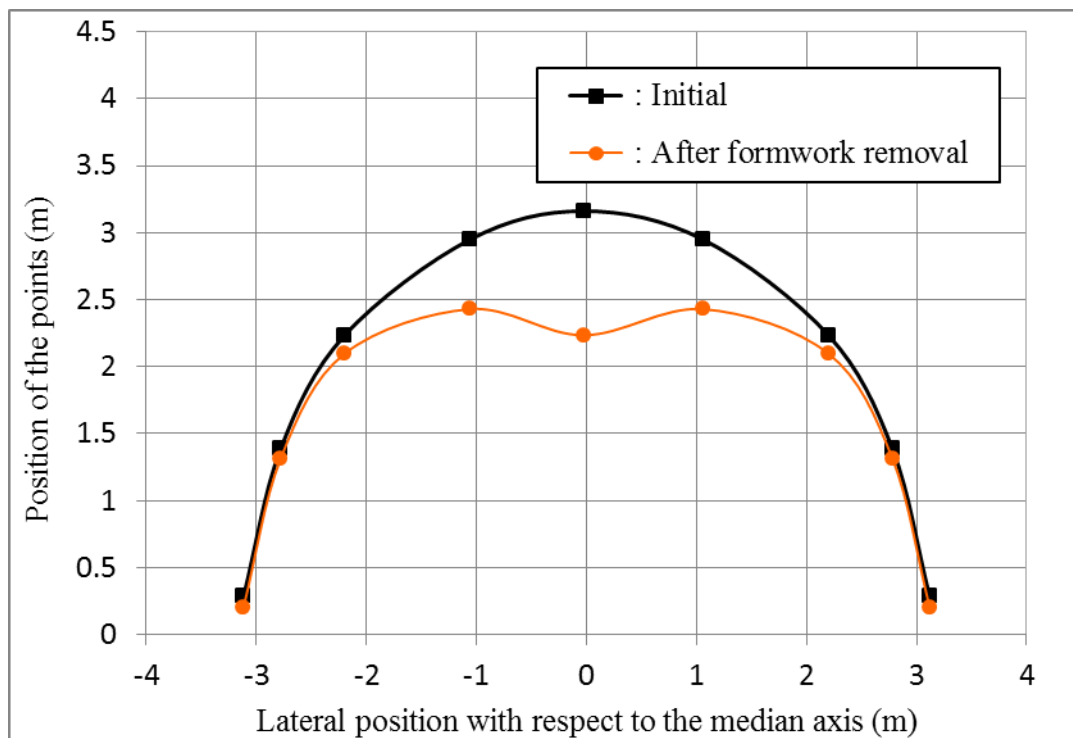


Figure 4: Displacement profile of the reflectors– displacement amplification factor: 1000.

The results show only micro-displacements of the haunches, while millimetre displacements are found elsewhere. The maximum vertical displacement, which is obtained for the keystone voussoir, is on the order of 1 mm, while the displacement of the arch haunches is at maximum 0.1 mm. At the keystone voussoir, a small horizontal shift to the right of 0.06 mm was measured. It may be due to the asymmetric shape of the abutments on each side of the bridge. Finally, the overall movement of the bridge when removing the formwork can be considered as insignificant. Nevertheless, one can note the singular behaviour of the keystone voussoir respectively to the adjacent voussoirs, and may gain better insight into the bridge behaviour.

### 3. DEM modelling

#### 3.1. Numerical model

A numerical modelling of the formwork removal is performed with the code *UDEC* [15], which works in plane-strain condition as standard mode. This code is a commercial software designed within the framework of the Discrete Element Method and has the ability to handle individual polygonal objects in interaction. The blocks can be considered either infinitely rigid or deformable, and the contact between two of them is supposed to be deformable. A mechanical law at contact is then defined. Here, a linear deformable contact is chosen and the possible slip between blocks is ruled by a Coulomb law. The influence of a mortar can be taken into account by means of cohesion within the contact law.

The actual system that must be modelled is a single-span arch stone bridge with a semi-circular arch. The arch is stabilised by two lateral spandrel walls that are more rigid than the other elements of the structure. They maintain an infill composed of untreated compacted gravel. Then, the whole system clearly works as a 3D system. Nevertheless, a plane-strain analysis within the plane of the spandrel walls is performed as a first attempt to understand the features observed during the formwork removal.

*Geometry:* Due to the symmetry of the system in the plane of the spandrel wall, just a half-bridge model is considered with the correct induced boundary conditions. The system then is composed of two different parts, the arch itself composed of well-adjusted wedged schist blocks (voussoirs) of good quality and the wall spandrel with schist blocks of lower mechanical strength. One can note in Figure 1 the paramount interlocking between the blocks of the vault and the block of the spandrel wall at the bottom. The aim is to rigidify the arch haunches and to allow a better transfer of horizontal loadings to the abutments and to the foundation. Thus, it incites not to consider the arch as a mechanically constant thickness vault and the extrados is supposed to encompass blocks that could be considered as a part of the spandrel wall. An empirical but mechanically plausible location of the extrados is proposed in Figure 5(a). For the sake of simplicity, the blocks belonging to the spandrel walls are chosen to be rectangular and of equal size. The arch and the spandrel wall lay on bedrock composed of larger blocks, which can be seen in Figure 3.

*Meshing:* The blocks are supposed to be deformable and a meshing must be associated to them. The density of meshes per voussoir is supposed to be large enough for a precise transfer of information from a voussoir to another one. Nevertheless, the average vault displacement field following the formwork removal was found little effect by the number of meshes (along the block height) chosen for the modelling. Nevertheless, in order to obtain a regular displacement field, the mesh number must be at least 3 along the considered contact height between two voussoirs. This contact height may be smaller than the total possible contact height, namely the total height of a voussoir. In this work, the typical number of meshes along the whole height of the keystone is equal to 20. The number of

meshes within the spandrel wall is chosen so that their density decreases according to the distance with respect to the closest voussoir 5(b)).

*Behaviour of blocks:* For the sake of simplicity, the blocks are supposed to behave like an isotropic material even if a schistosity can be observed on actual blocks. The direction of stresses is mainly perpendicular to the schistosity on site, and therefore the properties will be identified in that direction for the numerical study. The rocky blocks are supposed to behave like a linear elastic material, and thus a Poisson coefficient and a Young modulus need to be identified. Plasticity is not required at this level, because the formwork removal is not supposed to induce large stresses as it can be the case with life service loadings.

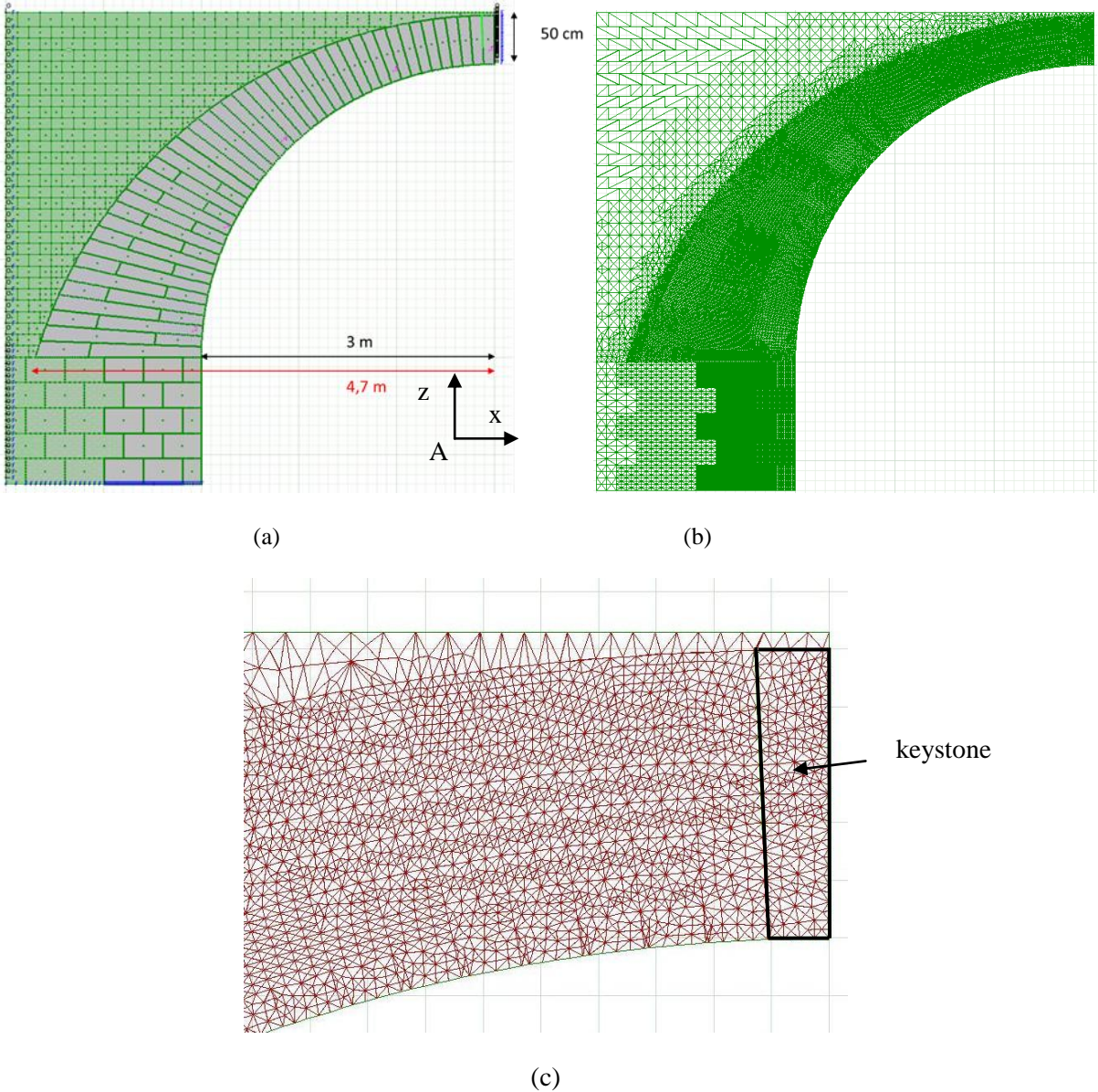


Figure 5: (a) Model of the half stone bridge, (b) Associated meshing, (c) Zoom of the keystone zone.

*Behaviour of the contact between blocks:* The contact (joint) between blocks is composed of two materials working as a parallel system. On one hand, irregularly extended and randomly placed

asperities that belong to two different blocks make contact between two adjacent blocks. On the other hand, a lime mortar which does not play a structural role fills the voids in between the asperities. This mortar being far more deformable than the asperities of the blocks the stresses mainly flow between blocks through the asperities.

The contact law between blocks involves a normal and a tangential stiffness. The possible influence of the mortar can nevertheless be taken into account. The Coulomb law requires the identification of the friction coefficient and the cohesion. The resistance of the contact to tension is supposed to be equal to zero.

*Boundary conditions:* The bedrock base is supposed to be fixed in all directions. The points along the vertical limits (abutment and keystone) can only move vertically.

### **3.2. Determination of the mechanical characteristics of the blocks**

The schists used for the bridge construction were extracted from local stone quarries that supplied material for the bridge construction. Some compression tests on schist blocks have been carried out in order to identify the Young modulus and the compressive strength of the two types of schists. Further tests were performed on a triplet of schist (three blocks bound by a lime mortar) to deduce the average behaviour of the contact blocks.

#### **3.2.1. Tests on schist samples**

Some compression tests on blocks of schist were performed mainly in order to identify the Young modulus of the material. Two types of schists were studied: the schist used for the voussoirs (type 1) and the one used for the spandrel walls (type 2), which is of lower quality. Six samples of type 1 denoted V1 to V6, and three samples of type 2 denoted W1 to W3 were tested. The samples of schist are solid cylinders with a diameter of about 60 mm. They were directly drilled on site within the stone quarries chosen for the bridge construction, and thus did not have exactly the same height. Extensometers were used to measure the strain in the central part of the sample (Figure 6(a)). The compression tests were performed in such a way that compression is directed perpendicularly to the schistosity planes, which also held true on site when the masons placed the different blocks.

For the schist of type 1, an average Young modulus of 53 000MPa was found with a standard deviation of 9 800MPa. The Young modulus for sample V6 was not measured due to an unexpected slippage of extensometers during the test. As an illustration, the stress-strain curves for sample V1 is given in Figure 7. The Young Modulus is measured after a first cycle (dotted line). The average compression strength for type 1 schist is equal to 126MPa with a standard deviation of 32MPa. For type 2 schist the Young modulus was found equal to 21 000MPa with a standard deviation of 7 300MPa and a compressive strength of 77MPa with a standard deviation of 8MPa. The mechanical properties of the schist stones are given in Table 1.

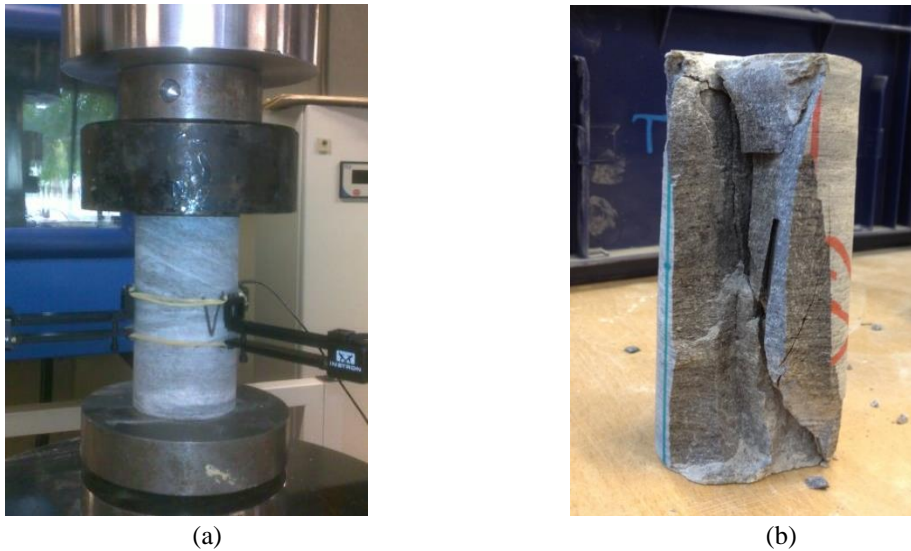


Figure 6: Compression test on a schist block: (a) test devices; (b) breaking mode of a sample.

Table 1: Mechanical properties of the schist stones (standard deviation is given within parentheses).

Schist type	Sample	Young modulus (MPa)		Compressive Strength (MPa)	
Type 1	V1	40 000		177	
	V2	50 000		141	
	V3	46 000	53 000	X	126
	V4	63 000	(9 800)	140	(32)
	V5	68 000		87	
	V6	X		142	
Type 2	W1	32 000		81	
	W2	19 000	21 000	84	77
	W3	12 000	(7 300)	65	(8)

### 3.2.2. Tests on masonry elements

Some compression tests on triplets of schist were performed in order to identify average properties of the contact surface between blocks and the underlying normal stiffness. Actually, the behaviour of an assembly of blocks depends on the behaviour of each block, on the behaviour of the contact zone which has specific properties, and possibly on the mortar binding the blocks. Compression tests on triplets, involving three blocks of schist bound by a lime mortar that merely fill the gaps between the blocks were performed. On Figure 8, the thickness of the joint and the mortar that can easily be seen is due to the fact that the block faces in contact are cut the same way it is done on-site, contrary to the other faces of the blocks which are cut using a circular saw. The induced roughness of the faces in contact creates a joint of about 1-cm thickness. The triplets have a rectangular shape with a total height of 20c m and a width of 10 cm to avoid buckling effects.

Since the average behaviour of the schist blocks was previously identified, these tests give the average behaviour of the contact zone between blocks and more specifically the normal stiffness of this zone.

Two triplets involving type 1 schist and one triplet with type 2 schist were tested (Figure 8). The results are given in Table 2.

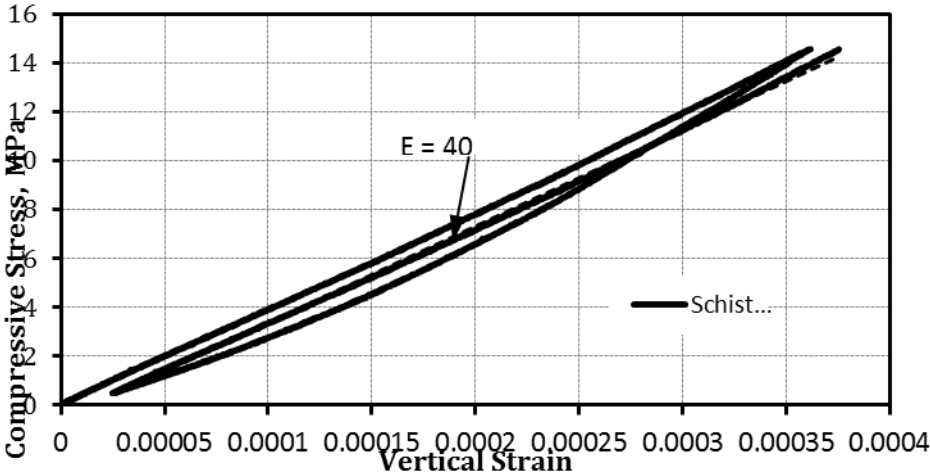


Figure 7: Loading and unloading compression tests on schist block of type 1.



Figure 8: Sample of a schist triplet after failure.

Table 2: Mechanical properties of the schist triplets (standard deviation is given within parentheses).

Material	Sample	Average Young Modulus (MPa)	Average Compressive Strength (MPa)
Type 1 Schist	VS1, VS2, VS3, VS4	4 400 (2 500)	54 (6)
Type 2 Schist	WS1, WS2, WS3	2 400 (1 200)	31(4)

The triplet for which the average normal stiffness of the contact zone between blocks is deduced is presented in Figure 8 and 9.

The three blocks were considered of the same properties and more specifically the same stiffness  $k_b$  and that the normal stiffness  $k_j$  of the two contact zones are equal. Actually with respect to compression, the triplet works as five materials of different stiffness placed in series.

The total stiffness of the triplet is denoted  $k_{eq}$ . The equation ruling the global behaviour of the triplet is then:

$$k_{eq}^{-1} = 3k_b^{-1} + 2k_j^{-1} \quad (1)$$

$k_{eq}$  and  $k_b$  have the dimension of a stress by unit length and can be found separately. We note  $E_t$  and  $E_b$  the global Young modulus of the triplet and of the schist material respectively. Then,  $k_{eq} = E_t / L_t$  and  $k_b = E_b / L_b$ . Finally, we obtain:

$$k_j = \frac{2k_b \times k_{eq}}{k_b - 3k_{eq}} \quad (2)$$

From the experimental results for the triplet using type 1 schist, the following data are obtained:  $E_b = 53000\text{MPa}$ ;  $L_b = 0.062\text{m}$ ,  $E_t = 4400\text{MPa}$ ,  $L_t = 0.186\text{m}$ . Therefore, the block stiffness (against compression), which is defined as the ratio between the Young modulus and the block length, can be derived. The stiffness of the triplet can be derived the same way. They are equal to  $850\text{GPa/m}$  and  $24\text{GPa/m}$ , respectively. According to Equation 2, the normal stiffness  $k_j$  of the contact zone between two blocks derived from the experiments, is equal to  $52\text{GPa/m}$ . This equation is one-dimensional and does not take into account the transversal influence of the block deformation on the interface behaviour, which is known to be negligible. For example, a DEM simulation of this test taking into account two-dimensional effects provided a normal stiffness  $k_j$  of the joint equal to  $51.7\text{GPa/m}$ , which is very close to  $52\text{GPa/m}$ .

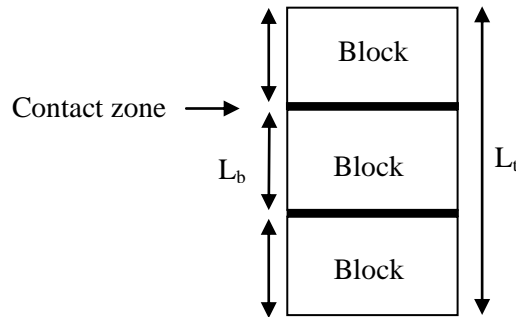


Figure 9: Actual triplet with the different entities.

Considering the average mechanical properties of the schist (Type 1 and 2) blocks derived from Table 1 as to the average size of the blocks, the average normal stiffness of the contact zone between two blocks are given in Table 4. The ratio between the tangential stiffness and the normal stiffness is taken equal to 0.8 [16]. A tilt test involving a schist block slipping on another schist block allowed the average friction coefficient of the contact zone of  $20^\circ$  to be obtained. The tensile strength of the contact is set to zero, whereas the cohesion is set to a very low value of  $10\text{Pa}$ .

The Young modulus was not identified and a Poisson ratio of 0.3 (typical measured for rocky stones) is considered.

Table 4: Properties of the blocks and of the contact zones between blocks.

		Type 1	Type 2
Blocks	Specific weight (kN/m <sup>3</sup> )	25	25
	Young modulus (MPa)	53 000	21 000
	Poisson ratio	0.3	0.3
Contact zone	Normal stiffness (GPa/m)	52	27
	Tangential stiffness (GPa/m)	41	21
	Friction coefficient (°)	20	20
	Cohesion (Pa)	10	10

### 3.3. Modelling of the formwork removal

Considering the properties defined previously and stating that the contact between the voussoirs involves the total lateral height of the voussoirs, the 2D simulation of the formwork removal was performed. The simulation does not consider the real process, but rather an approximated and simpler one. The gravity is imposed in successive stages from zero to the actual value of 9.81 m/s<sup>2</sup> within five steps in order to ensure that the static equilibrium is obtained more quickly. The equilibrium is supposed to be obtained when the ratio of the average unbalanced mechanical force magnitude divided by the average applied mechanical force magnitude for all block centroids or gridpoints in the model reaches 10<sup>-5</sup> at the end of each stage of gravitational acceleration increase. This ratio is eventually set to 10<sup>-6</sup> for the achievement of the final equilibrium.

The initial position of the arch (gravity equal to zero) is given in Figure 10 together with the arch vertical displacement field obtained by the simulation. In that figure, an amplification factor of 1000 is given for the vertical displacement field. The vertical displacement field obtained by measurements on-site during the actual formwork removal is also given. The magnitude of displacements found by the simulation is in the order of magnitude of the displacements found on site. Nevertheless, the peculiar displacements of the voussoirs within the keystone zone could not be obtained. In the proposed model, the stress flows from one voussoir to another one by the total voussoir height. It underlies that contact points or contact length zones between two voussoirs are uniformly distributed along the total lateral surface of the voussoir, which is not the case on site because the rubble masonry uses un-hewn building stones with a low strength mortar. The stress field found by the simulation is given in Figures 11(a) and (b). In these figures, a positive stress denotes tension. The materials mainly face compressive stresses, which was expected, but some blocks also face some tensile stresses.

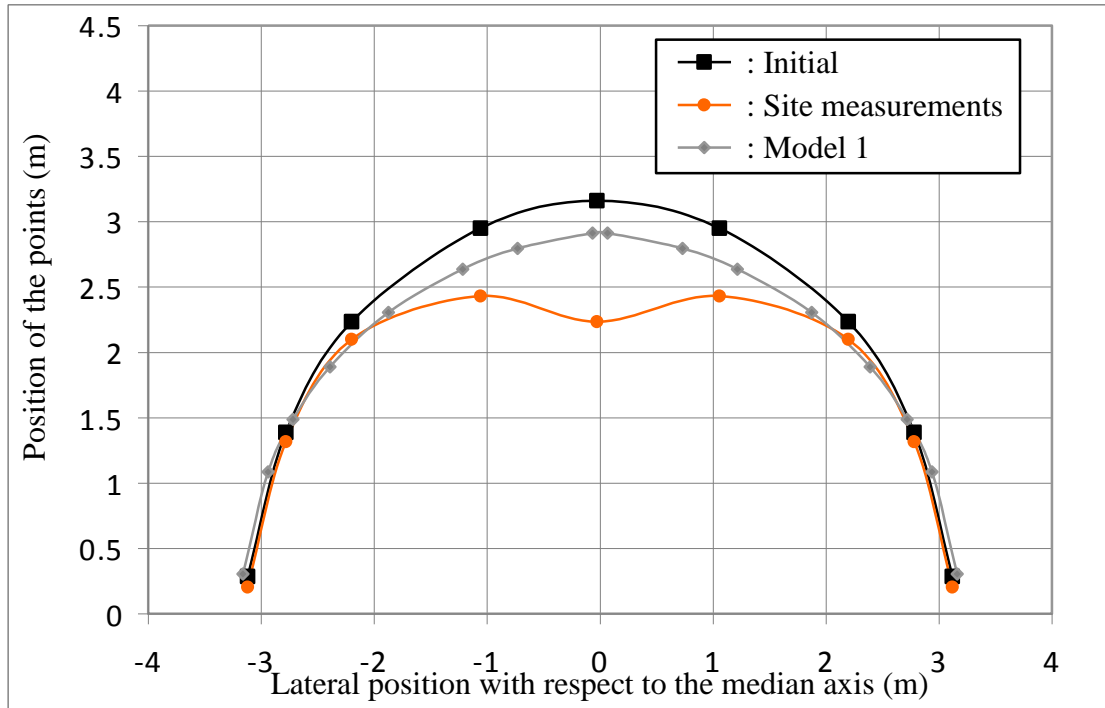


Figure 10: Vertical displacement field obtained by simulation and on site following the formwork removal; contact length involving the keystone: 100%. Amplification factor for displacements: 1000.

Actually, the voussoirs are manually placed on the formwork without any other device except for the keystone voussoir. This latter is manually thrust with a sledge hammer between the two adjacent voussoirs. The gradual insertion of the keystone between the adjacent blocks is made possible by the progressive damage of the contact points and surfaces. It seems that before the formwork removal, the contact points or contact surfaces were not homogenously distributed along the total lateral surface of the keystone voussoir, but mainly in the bottom part of it (close to the arch intrados). It also seems that during the formwork removal, there is a change of the location for contact between the keystone voussoir and the adjacent voussoirs. The contact zone seems to shift towards the extrados.

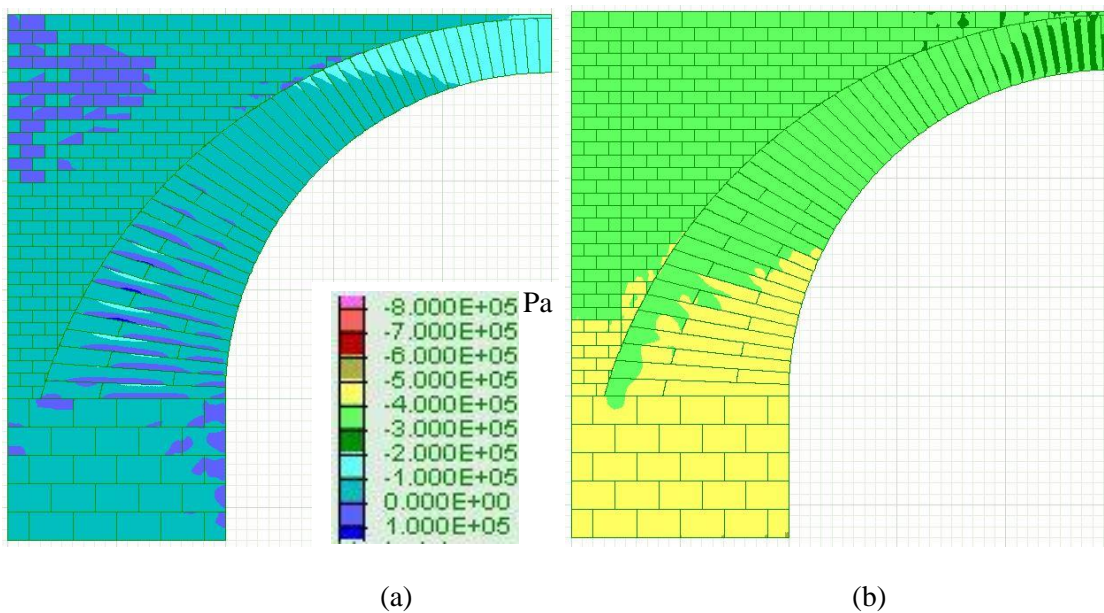


Figure 11: Stress field after the formwork removal, Model 1; (a): horizontal stress, (b): vertical stress.

Considering this observation, a new simulation is performed. Here, the contact zone of the keystone voussoir with the adjacent voussoirs is extended along the 20% of the total possible contact zone and at the bottom part of the lateral voussoir surface. This is performed by creating a crack extending along the 80% of the upper part of lateral voussoir surface, avoiding possibilities for contacts in that zone at the initial state (before formwork removal). This new model for the system is denoted “Model 2” (Figure 12(b)). Model 1 is given in Figure 12(a) as a reference. During the formwork removal, contacts in that zone can eventually be created as the opposite sides of the cracks may get closer one to the other one. The result of the simulation is given in Figure 13. The vertical displacement field qualitatively shows the peculiar pattern observed on-site, which tends to validate the initial statement.

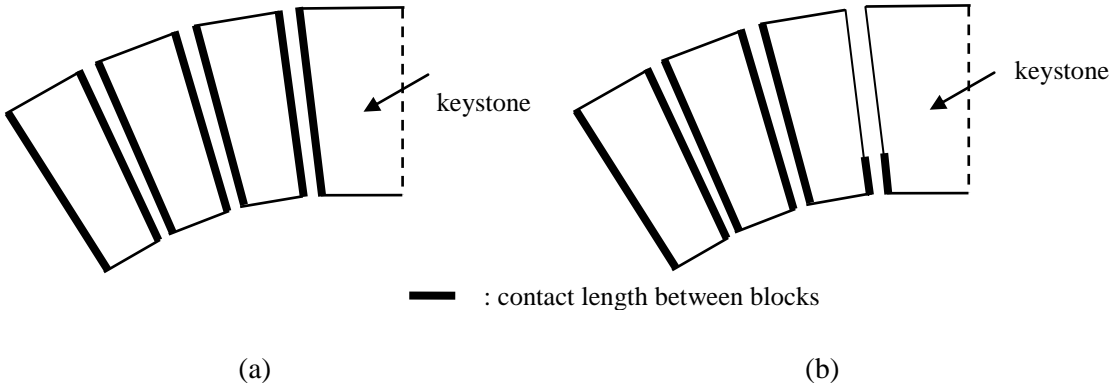


Figure 12: Contact length of the keystone with the adjacent voussoir; (a): Model 1, full length, (b): Model 2: 20% total length

Figure 14(a) and (b) give the local displacement field of each block. The linear displacements for each node within the blocks are given in Figure 14(a) while the rotation of a block is given by an angular sector with amplitude related to the magnitude of the rotation in Figure 13(b). The movement of the blocks does not take place by slippage between adjacent voussoirs, but merely by rotation around axis (Oy), behaviour well known for vault masonries.

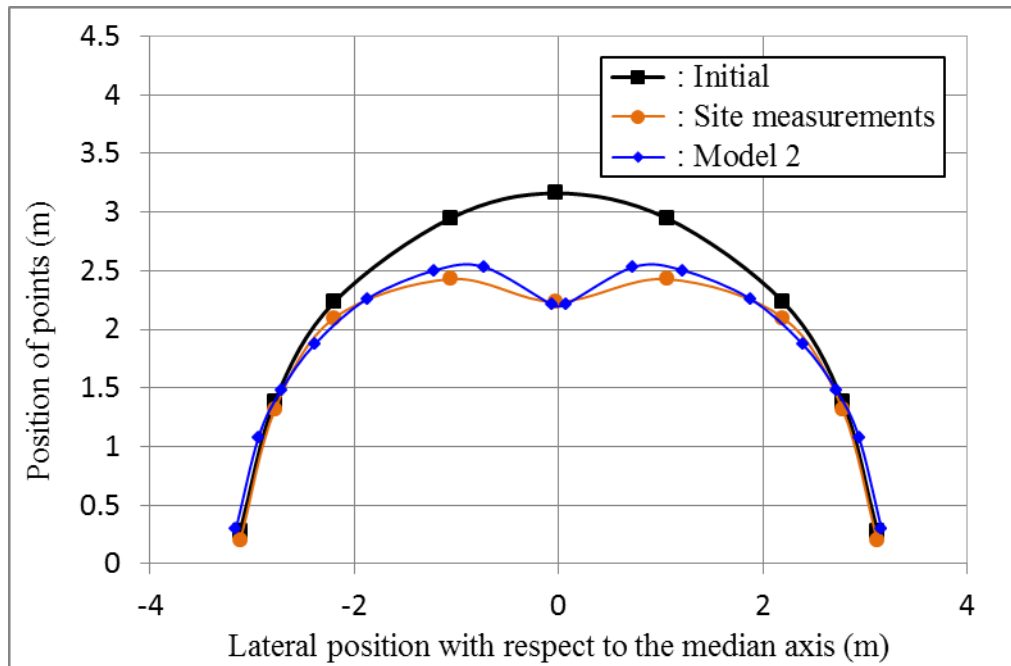


Figure 13: Vertical displacement field obtained by simulation and on site following the formwork removal, contact length involving the keystone: 20%. Amplification factor for displacements: 1000.

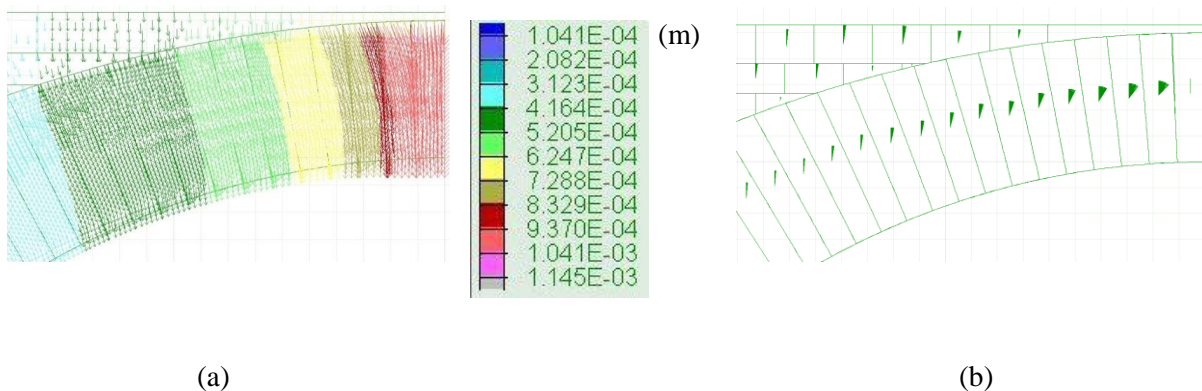


Figure 14: Local displacement fields within the keystone zone, Model 2; (a): linear displacement of nodes, (b) average rotation of blocks (maximum value  $0.04^\circ$ ).

Figures 15(a) and (b) give the stress field obtained after the formwork removal using Model 2. The scale of stress is the same as the one chosen in Figures 11(a) and (b) when using Model 1. The reduction of the contact length affects the distribution of stresses in a large number of the voussoirs close to keystone. The maximum stress which is nearly five times larger than for Model 1 within the keystone is not at the intrados, but at a point above the intrados and the contact length increased from 20% to nearly 50% in Figure 15(a). Indeed, compressive stresses flow along this distance between the keystone and the adjacent voussoir after the formwork removal. One can note that the maximum compressive stress is equal to 800kPa, which is much smaller than the maximum compressive strength of the material (about 130MPa). It justifies the hypothesis of elastic behaviour taken in the simulations.

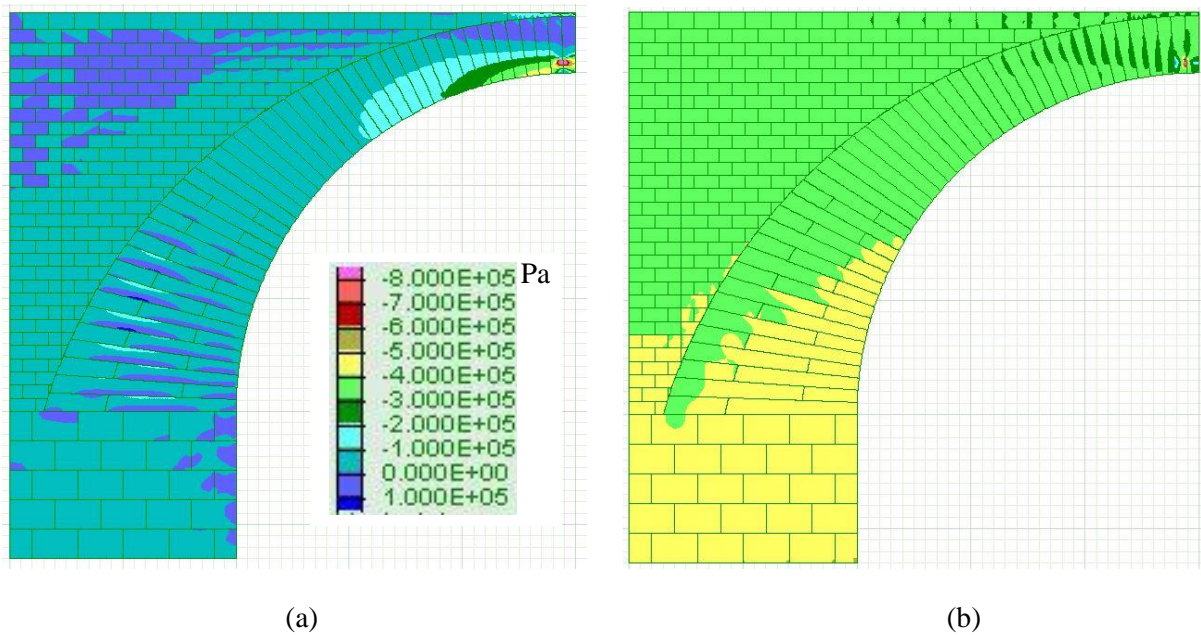


Figure 15: Stress field after the formwork removal, Model 2; (a): horizontal stress, (b): vertical stress.

Finally, the sharp discontinuity of the simulated displacements (keystone compared to adjacent voussoirs) may be due to the fact that only the extent of the contact zone related to the keystone voussoir was changed. The reduction of the extent of the contact zone in the bottom lateral zone of the voussoir may also hold true for adjacent voussoirs. Consequently and in a same way, the extent of the contact zone for the contact surfaces involving all the contact zones of the voussoirs adjacent to the keystone voussoir was reduced. Therefore, Model 3 denotes the model where all the contact zones of the keystone and the voussoir adjacent to the keystone were affected by the surface reduction, Model 4, when this reduction affects the two adjacent voussoirs (in the same half system). The significance of models  $i$  involved in the figures is illustrated in Figure 16 and summarized in Table 5 for convenience. The results for these new models are given in Figure 17.

The reduction of the contact length for the voussoir adjacent to the keystone (Model 3) induces a slight downward shift of the latter one and equal shifts for the other voussoirs. Model 4 does not induce a further movement of the keystone, but slightly reduces the gap between the displacement magnitude of the keystone and the displacement of the adjacent voussoirs. Then a better forecast of actual displacements of the arch would encompass a modelling involving a reduction of the extent of the contact length for at least two voussoirs adjacent to the keystone.

Actually, the precise forecast of the actual displacements is difficult to achieve since both the number of voussoirs involved in the reduction of contact length and the general extent of this reduction play the same role though the second one seems to be more critical. As an illustration of this statement, Figure 18 shows the displacement field of the voussoirs involving three different reductions of contact length for the keystone (Model 2). In this figure, if the surface of contact is only of 40% of the total keystone height, the displacement field is still close to the one observed when the total lateral voussoir height is considered for the transfer of stresses in the joint. Moreover, the reduction of the contact zone extent amplifies the gap between the displacement of the keystone and the displacement of the adjacent voussoirs. This gap is due to a larger rotation of the adjacent voussoirs with respect to the keystone which is facilitated if the contact length is reduced. Therefore, a reduction of 20% is a first proposal.

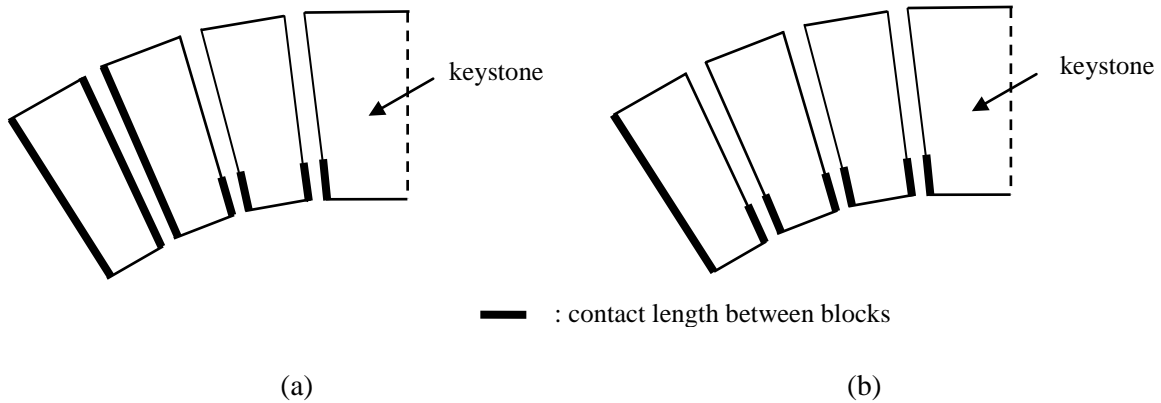


Figure 16: Contact length between the voussoirs, by default full length; (a): Model 3, 20% total length for contacts involving the keystone and the voussoir next to the keystone (b): Model 4: 20% total length for contacts involving the keystone and the two voussoirs next to the keystone.

Table 5: Type of model and significance.

Modelling	Significance
1	Contact length on the overall lateral surface for all the voussoirs
2	Contact length reduced to 20% for the keystone
3	Contact length reduced to 20% for the keystone and for the adjacent voussoir
4	Contact length reduced to 20% for the keystone and for the two adjacent voussoirs

The difficulty to obtain a precise forecast arises from the exact location of the contact zone, which may not start from the very intrados but nearby, and that can differ for each joint. One may also claim that the value for the reduction of contact length may be different for each joint. To conclude, at this point there is too little information to state which scenario is closer to what occurred on site. A further on-site measurement when loading the bridge to typical service life loadings is likely to help in this respect providing further information.

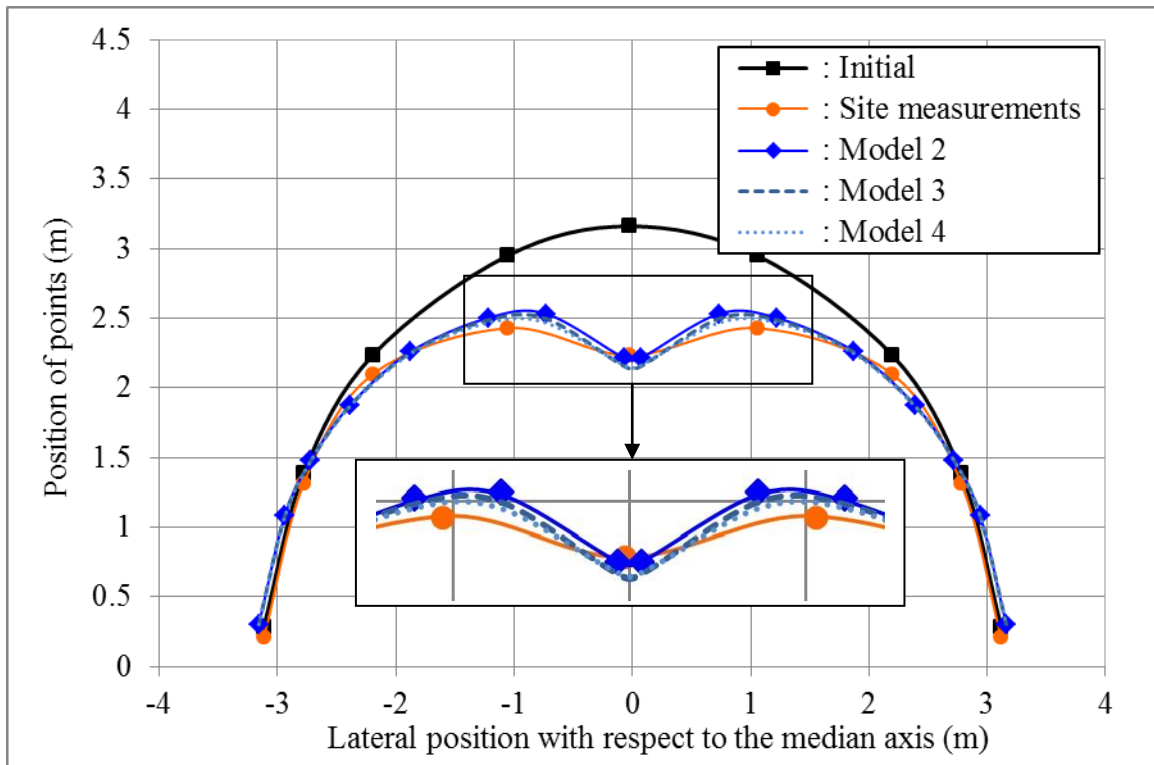


Figure 17: Vertical displacement field obtained by simulation and on site following the formwork removal; the significance of the different models is given in Table 5. Amplification factor for displacements: 1000.

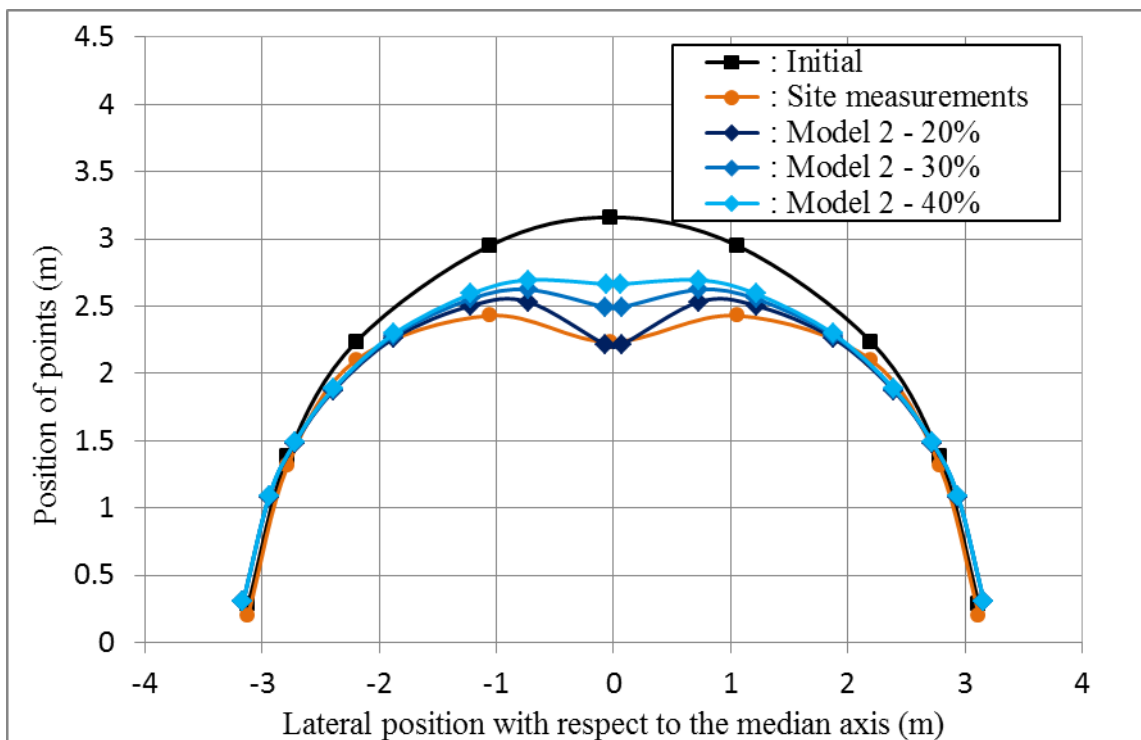


Figure 18: Vertical displacement field obtained by simulation following the formwork removal, influence of the extent of the contact zone. Amplification factor for displacements: 1000.

#### **4. Conclusions**

On-site measurements of the displacements of a masonry bridge with blocks weakly bound by a lime mortar were performed at the stage of the formwork removal. The maximum displacement under its own weight was found on the order of 1 mm and took place at the keystone voussoir. The displacements field showed a singular profile with a singularity for voussoirs very close to the keystone. It seems that before the formwork removal, the contact points between the voussoirs did not extend uniformly on the whole geometrical lateral surfaces of the blocks, but just along a reduced zone located at the bottom part of them. When the formwork was removed, an upward shift of the contact zone may have occurred. The key mechanism here is the permitted rotation of a voussoir with respect to another one that would have not been triggered if the contact length would have involved the total lateral surface of the joints.

A 2D numerical analysis of the formwork removal using a discrete element method was proposed to provide better insight on mechanisms that took place on site. The parameters of the mechanical laws were identified by experimental tests including compression tests on schists and triplets. A first model showed that if the contact zone between blocks involves the whole lateral height, the pattern observed on-site cannot be found.

The reduction of the extent of the contact zone between the voussoirs enabled finding the peculiar displacement field observed on-site. This feature would not have been found using a finite element method, and even if the range is very small of involved displacements, it helps to have a better insight into the transfer of stresses within the arch. The reduction must be settled to a value close to 20%, which is important. It implies that larger-than-expected local stresses may exist within the voussoirs. This reduction must affect not only the contact zone between the keystone and the adjacent voussoirs, but at least two adjacent voussoirs on each side of the keystone. Moreover, the zone of contact may not be strictly located at the bottom part of the voussoir, but in a zone slightly above.

The detailed forecast of the displacement field was beyond the scope of this study, but further on-site measurements involving loadings typical of the service life of this kind of bridge will help to precise this study that must be considered as a first attempt to understand the behaviour of Chaldecoste bridge.

#### **Acknowledgements**

The present work is part of the research project C2D2 10 MGC S 01 denoted PEDRA (Behaviour of dry stone or weakly bound structures) funded by the Ministry of Ecology (MEDDE) and the Civil and Urban Engineering Network (RGCU). The Région Rhône-Alpes founded a Fellowship CMIRA for JC Morel for 5 months in Bath University. The authors want to thank these institutions for their financial support. Authors would also like to thank, Joachim Blanc-Gonnet, Stéphane Cointet and the group of artisan-builders who built the bridge: Thomas Brasseur, Marc Dombre, Bruno Durand and Christian Emery for their technical support.

#### **References**

- [1] Gilbert M, Melbourne C. Rigid-block analysis of masonry structures. *Structural Engineering* 1994; 72:356-61.
- [2] Oliveira DV, Lourenço PB, Lemos C. Geometric issues and ultimate load capacity of masonry arch bridges from the northwest Iberian Peninsula. *Engineering Structures* 2010; 32(12):3955-3965.
- [3] Colas AS, Morel JC, Garnier D. 2D modelling of a dry joint masonry wall retaining a pulverulent backfill. *International journal for numerical and analytical methods in geomechanics* 2010; 34:1237-1249.
- [4] Fanning PJ, Boothby TE. Three-dimensional modelling and full-scale testing of stone arch bridges. *Computers and Structures* 2001; 79:2645-2662.
- [5] Toker S, Unay AI. Mathematical modeling and finite element analysis of masonry arch bridges. *Journal of Science* 2004; 17(2):129-139.
- [6] Cavicchi A, Gambarotta L. Two-dimensional finite element upper bound limit analysis of masonry bridges. *Computers and Structures* 2006; 84:2316-2328.
- [7] Audenaert A, Fanning P, Sobczak L, Peremansa H. 2-D analysis of arch bridges using an elasto-plastic material model. *Engineering Structures* 2008; 30:845-855.
- [8] Sevim B, Bayraktar A, Altunisik AC, Atamturktur S, Birinci F. Finite element model calibration effects on the earthquake response of masonry arch bridges. *Finite element in Analysis and Design* 2011; 47:621-634.
- [9] Domede N, Sellier A, Stablon T. Structural analysis of a multi-span railway masonry bridge combining in situ observations, laboratory tests and damage modelling. *Engineering Structures* 2013; 56: 837-849.
- [10] Toth AR, Orban Z, Bagi K. 2009. Discrete element analysis of a stone masonry arch. *Mechanics Research Communications* 2009; 36: 469- 480.
- [11] Rafiee A, Vinches M, Bohatier C. Application of the NSCD method to analyse the dynamic behaviour of stone arched structures. *Int J Solids Struct*, 2008; 45:6269-83.
- [12] Sousa Gago A, Alfaiate J, Lamas A. The effect of the infill in arched structures: Analytical and numerical modeling, *Engineering Structures* 2011; 33(5):1450-1458.
- [13] Rafiee A, Vinches M. Mechanical behaviour of a stone masonry bridge assessed using an implicit discrete element method. *Engineering Structures* 2013; 48:739-749.
- [14] Thavalingam A, Bicanic N, Robison JJ, Ponniah DA. Computational framework for discontinuous modelling of masonry arch bridges. *Comput Struct* 2001; 79:1821-30.
- [15] Itasca Consulting Group, Inc., 2011, UDEC (Universal Distinct Element Code), Version 5.0, Minneapolis, MN: ICG.
- [16] Mindlin RD. Compliance of Elastic Bodies in Contact. *Journal of Applied Mechanics* 1949; 16:259-268.